Vol. 35 (2004) ACTA PHYSICA POLONICA B No 9

BETHE PLOTS AND NEUTRON HALO*

Andrzej Baran and Paweł Mierzyński

Institute of Physics, M. Curie-Skłodowska University
pl. M. Curie-Skłodowskiej 1, 20-031 Lublin, Poland

(Received May 11, 2004)

The relative excess of a neutron density introduced by Bethe is applied to classify atomic nuclei with respect to a neutron halo. Calculations are based on the relativistic mean field model and are performed for 116 spherically symmetric nuclei across the periodic system of elements and for a group of deformed nuclei studied in antiproton annihilation reaction at the LEAR facility in CERN. Basic properties of the neutron excess function are discussed.

PACS numbers: 21.10.Ma, 24.10.Jv, 21.10.Jz, 21.10.Ft

In the early 1970' Bethe [1] introduced a function

$$\delta_{\mathrm{B}} = \frac{Z}{N}\rho_N - \rho_Z = \tilde{\rho}_N - \rho_Z \,, \tag{1}$$

which describes the difference of the relative neutron density $\tilde{\rho}_N = Z/N\rho_N$ and the density of protons ρ_Z in the nucleus. The integral of δ_{B} over the whole space equals to zero

$$\int \delta_{\mathrm{B}}(r)\, d^3r = \frac{Z}{N}\int \rho_N(r)\, d^3r - \int \rho_Z(r)\, d^3r = 0\,. \tag{2}$$

This rather trivial property of the neutron excess function makes it very interesting and allows to define easily the total peripheral neutron excess without the knowledge of the density distribution in the nuclear periphery.

* Presented at the XXVIII Mazurian Lakes School of Physics, Krzyże, Poland, August 31–September 7, 2003.

To see this let us consider the case of a spherically symmetric nucleus with some mean radius R. The integral in Eq. (2) can then be written as

$$\begin{aligned} 0 \;&=\; \int \delta_{\mathrm{B}}(r)\, d^3r = 4\pi \int\limits_0^\infty \delta_{\mathrm{B}}(r) r^2\, dr \\ &=\; 4\pi \int\limits_0^R \delta_{\mathrm{B}}(r) r^2\, dr + 4\pi \int\limits_R^\infty \delta_{\mathrm{B}}(r) r^2\, dr \end{aligned} \tag{3}$$

which means the absolute equality of integrals in the last expression *i.e.*,

$$4\pi \int\limits_0^R \delta_{\mathrm{B}} r^2\, dr = -4\pi \int\limits_R^\infty \delta_{\mathrm{B}} r^2\, dr\,, \tag{4}$$

where the choice of R is arbitrary. Let us define the following function of r

$$I_{\mathrm{B}}(r) = -4\pi \int\limits_0^r \delta_{\mathrm{B}}(r') r'^2\, dr' = 4\pi \int\limits_r^\infty \delta_{\mathrm{B}}(r') r'^2\, dr'\,. \tag{5}$$

We will assume R to be equal to a root R_δ of the $\delta_{\mathrm{B}}(r)$ function which is closest to the nuclear radius $R = r_0 A^{1/3}$ (see *e.g.* [2]), where A the nuclear mass number and r_0 is the nuclear radius constant. The value of $I_{\mathrm{B}}(r)$ calculated at the $r = R_\delta$ we call the outer neutron excess and denote by $\varDelta_{\mathrm{B}}$

$$\varDelta_{\mathrm{B}} \equiv I_{\mathrm{B}}(R_\delta)\,. \tag{6}$$

The value of $\varDelta_{\mathrm{B}}$ gives also the total relative proton excess inside the nucleus or the relative neutron deficit in the nuclear interior. It follows from Eq. (4) that the integral describes the relative excess of neutrons outside of the nucleus. In the model case of sharp density distributions of both neutrons and protons with equal radii ($R_Z = R_N = R$) δ_{B} function disappears at each point r and the outer neutron excess is equal to zero as it should.

An example of the δ_{B} function is shown in Fig. 1 for ^{208}Pb. The neutron excess function has a root R_δ which is very close to the value of $R_{1/2}$ at which the density of the nucleons falls to the half of its average internal value. The zero of the δ_{B} function is at $r \approx 6.5$ fm and is also close to the nuclear radius $R = 7.3$ fm. The maximum of $\delta_{\mathrm{B}}(r)$ corresponding to $r > R$ appears approximately at $R + 1.5$ fm.

The corresponding $I_{\mathrm{B}}(r)$ integral as a function of r is plotted in figure 2. At $r = R_\delta = 6.50$ fm *i.e.*, at the root of the Bethe function has its maximum and goes to zero at $r \to \infty$.

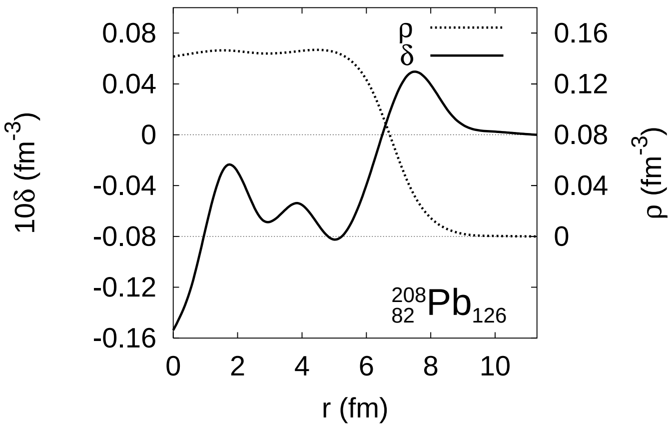

Fig. 1. Bethe function $\delta_{\rm B}(r) = (Z/N)\rho_N - \rho_Z$ (solid line) for ^{208}Pb. The solid line shows the total density $\rho_n + \rho_Z$ (see the similar plot in Ref. [1]).

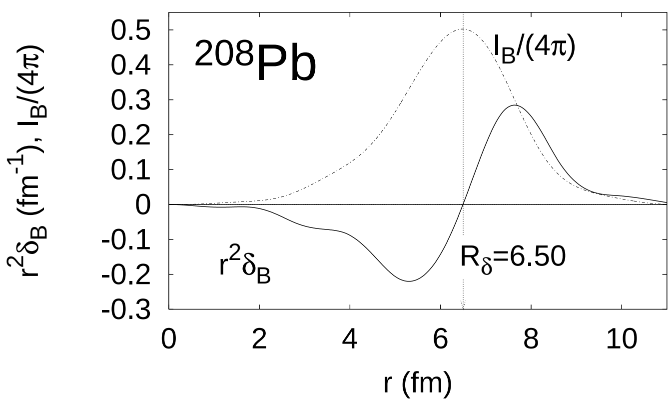

Fig. 2. Integral $I_{\rm B}$ of Bethe neutron excess function $I_{\rm B}(r)$ (dashed line) as a function of r for ^{208}Pb. The point R_δ is the root of the $\delta_{\rm B}$ and maximum of the function $I_{\rm B}(r)$. The maximal value of $I_{\rm B}$ defines the outer neutron excess $\varDelta_{\rm B}$. Solid curve represents $r^2\delta_{\rm B}(r)$.

In the present paper we consider 116 spherically symmetric nuclei taken from Ref. [3] for which we calculate Bethe functions and the corresponding neutron excess integrals in the relativistic mean-field theory. Next we report the results of the calculations and discuss its consequences for determining the peripheral or halo properties of nuclei.

To determine the nuclear densities we use the relativistic mean field theory (RMF) (see *e.g.*, [4, 5] based on the following Lagrangian density

$$\begin{aligned}\mathcal{L} = {} & \bar{\psi}_i\{i\,\gamma^\mu\,\partial_\mu - m\}\psi_i \\ & +\frac{1}{2}\partial^\mu\sigma\,\partial_\mu\sigma - \frac{1}{2}m_\sigma\sigma^2 - g_\sigma\,\bar{\psi}_i\psi_i\,\sigma - \frac{g_2}{3}\sigma^3 - \frac{g_3}{4}\sigma^4 \\ & -\frac{1}{4}\Omega^{\mu\nu}\,\Omega_{\mu\nu} + \frac{1}{2}m_\omega^2\,\omega^\mu\omega_\mu - g_\omega\,\bar{\psi}_i\,\gamma^\mu\,\psi_i\,\omega_\mu \\ & -\frac{1}{4}\vec{R}^{\mu\nu}\vec{R}_{\mu\nu} + \frac{1}{2}m_\rho^2\,\vec{\rho}^{\,\mu}\vec{\rho}_\mu - g_\rho\bar{\psi}_i\,\gamma^\mu\vec{\tau}\,\psi_i\,\vec{\rho}_\mu \\ & -\frac{1}{4}F^{\mu\nu}F_{\mu\nu} - e\bar{\psi}_i\,\gamma^\mu\,\frac{(1-\tau_3)}{2}\,\psi_i\,A_\mu\,. \end{aligned} \tag{7}$$

The fields belong to the nucleon (Dirac spinor field ψ), the low mass isovector–vector meson ($\vec{\rho}_\mu; \vec{R}_{\mu\nu}$), the isoscalar–vector ($\omega_\mu; \Omega_{\mu\nu}$), scalar σ and to the massless photon vector field ($A_\mu; F_{\mu\nu}$).

The Dirac spinors ψ_i of the nucleon and the fields of the σ, ρ and ω mesons as well as the electromagnetic field A_0 are the solutions of the coupled Dirac, Klein–Gordon and Maxwell equations which are obtained from the Lagrangian (7) by means of the classical variational principle.

Hereby we use the following Lagrangian parameters [6] $m = 939$ MeV, $m_\sigma = 508.194$ MeV, $m_\omega = 782.501$ MeV, $m_\rho = 763.000$ MeV and the coupling constants $g_\sigma = 10.217$, $g_\omega = 12.868$, $g_\rho = 4.474$, $g_2 = -10.431$ fm^{-1}, $g_3 = -28.885$. In the spherical case we used the simplified phenomenological average pairing gap $\Delta = 12/\sqrt{A}$, where A is the atomic number.

The calculations of Δ_{B} were done for 116 spherically symmetric nuclei and, in addition, for a nine deformed nuclei studied in Refs. [7, 8].

The spherically symmetric nuclei for which we calculated the Bethe function are shown in Fig. 3. The information on the sphericity of these nuclei is drawn from Ref. [3]. The majority of nuclei shows a large global neutron excess $I = (N-Z)/A$.

The tin isotopes are experimentally known to cover the whole range of N from magic $N = 50$ to the magic number $N = 82$. The outer excess δ_{B} together with the total density distributions are shown in figure 4 for the chain of tin isotopes. One observes an increasing bump of the Bethe δ_{B} function with increasing N in the outer nuclear region ($r > R$).

In figure 5 we have shown the outer neutron excess Δ_B as function of the mass number A for all considered nuclei. Only a small group of nuclei in the vicinity of $A = 40$ shows a negative outer neutron excess Δ_{B} indicating a peripheral proton excess. There are also nuclei for which the outer proton and neutron distributions are nearly equal. This is mainly the case for nuclei with $A < 100$ and $N \approx Z$.

The following nuclei were studied in annihilation reactions of antiprotons with nucleons in the peripheral region of the nucleus [7, 8]: ^{58}Ni, ^{96}Zr, ^{96}Ru,

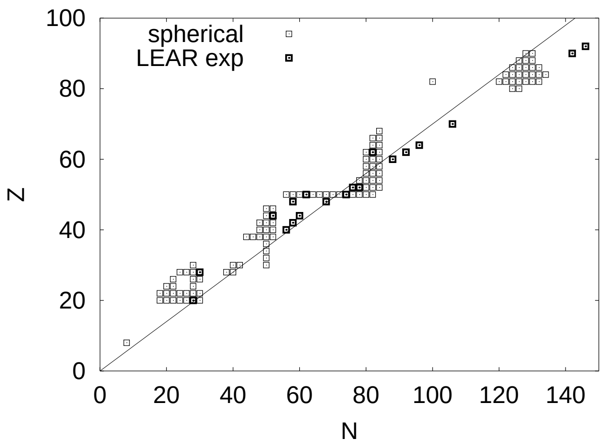

Fig. 3. Spherically symmetric nuclei (thin squares) as well as LEAR experiment (deformed) nuclei (thick line squares). The information on the sphericity is drawn from Ref. [3]. The dashed line approximates β-stability line.

^{130}Te, ^{144}Sm, ^{154}Sm, ^{176}Yb, ^{232}Th, ^{238}U. The authors of the cited papers introduced the halo factor

$$f \sim \frac{Z}{N}\frac{\sum_s \Gamma_n^s}{\sum_s \Gamma_p^s}\,, \tag{8}$$

where the antiproton absorption width Γ_n^s (Γ_p^s) on nuclear neutrons (protons) is defined by

$$\Gamma_{n(p)}^s \sim \int \rho_{n(p)}\,|\Psi^s(r)|^2\,P(r)\,r^2\,dr\,. \tag{9}$$

Here $\Psi^s(r)$ is the antiproton wave function and $P(r)$ is a geometric factor.

In RMF calculations for the deformed systems we used the realistic pairing gap energies $\Delta^{(3)}$ (see *e.g.* Ref. [9]) calculated from experimental masses. We slightly modify the procedure of determining the outer neutron excess $\Delta_{\rm B}$ since it is hard to find numerically the roots of $\delta_{\rm B}(\vec{r})$ which form a complicated surface. The new $\Delta_{\rm B}$ is defined as the maximal value of the integral

$$\Delta_{\rm B}(R) = -\int\limits_{V_R} d^3\vec{r}\delta_{\rm B}(\vec{r})\,, \tag{10}$$

where V_R is the volume enclosed by the sphere of radius R. Both procedures produce nearly the same results in the case of spherical nuclei.

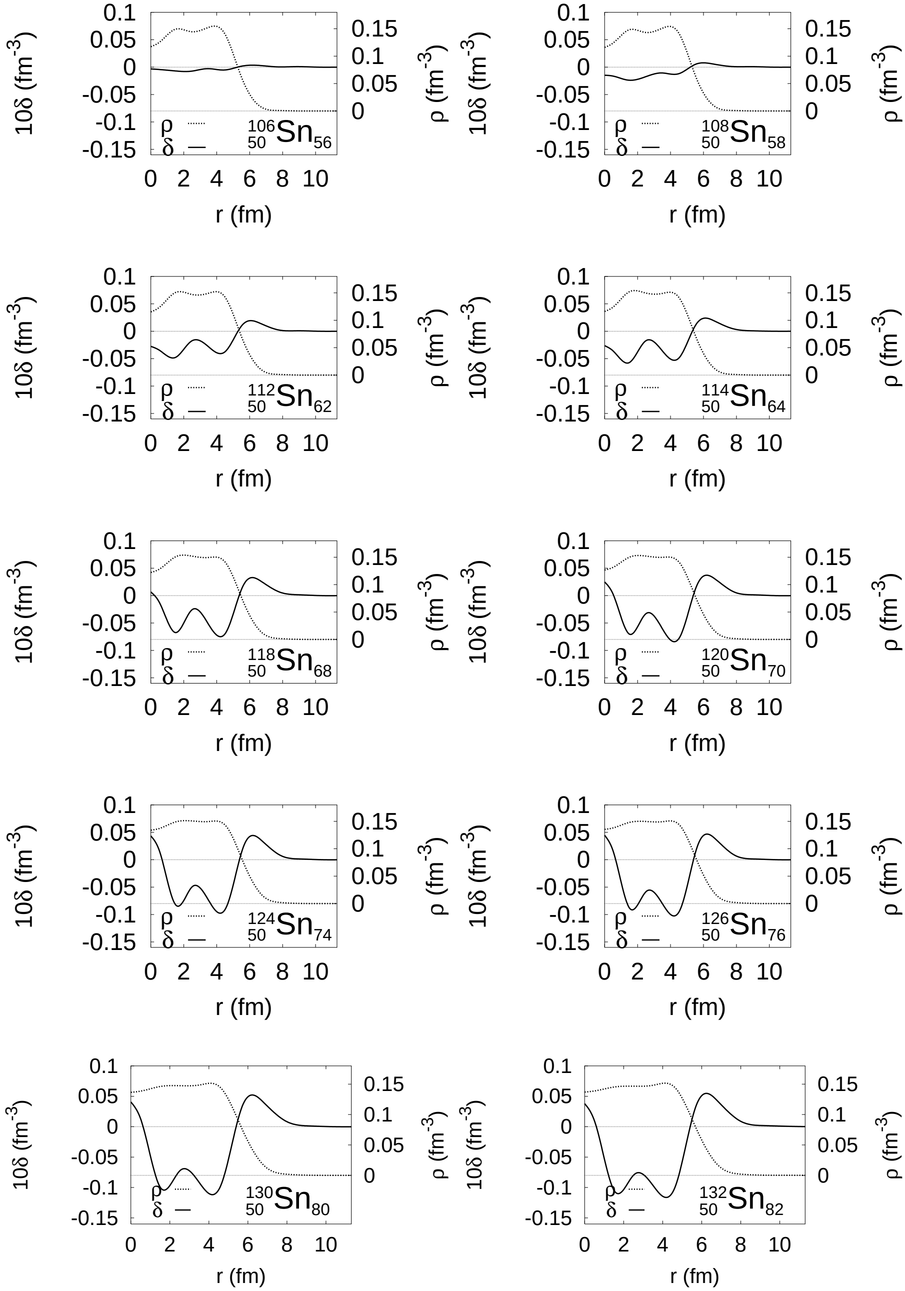

Fig. 4. Relative neutron excess function δ_{B} for tin (Sn) isotopes as a function of r.

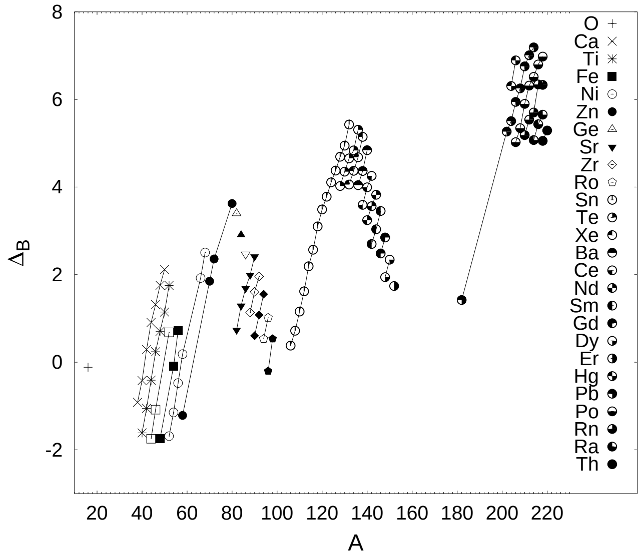

Fig. 5. Neutron excess function Δ_{B} for spherical nuclei *vs* mass number A.

In Table I are shown for these nuclei the values of the outer neutron excess Δ_{B}, the experimental halo factors f_{exp} deduced from the experimental data on antiproton annihilation and the halo factors f_{RMF} calculated in the RMF model (see Ref. [10]). One can observe a positive correlations between the factor f_{exp} of Ref. [7, 8] and the outer neutron excess Δ_{B} studied here. This is also shown in figure 6.

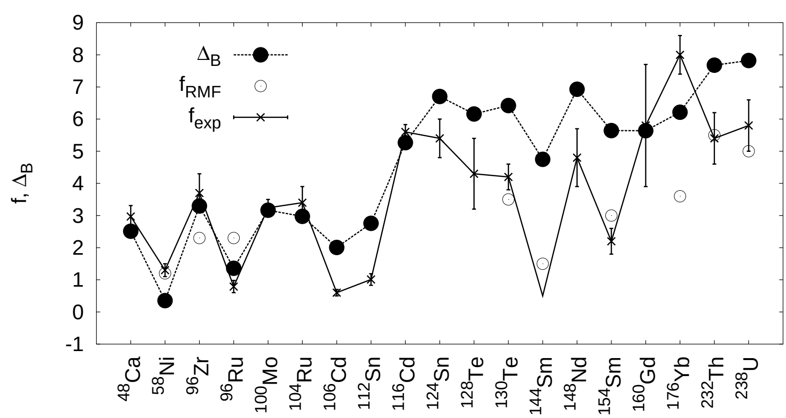

Fig. 6. The different halo indicators: the experimental halo factor of Ref. [7, 8], halo factor f_{RMF} (circles) and the outer neutron excess Δ_{B} (full circles). The factor f_{RMF} was taken from Ref. [10].

TABLE I

Experimental (second column) and theoretical (3rd column) halo factors f and Bethe outer neutron excess integral (third column) calculated in RMF model with NL3 set of parameters. The experimental values are taken from Ref. [7, 8]. The theoretical values are calculated in Ref. [10]

Nucleus	$f_{\rm expt}$	$f_{\rm RMF}$	$\Delta_{\rm B}$
^{48}Ca	2.97	—	2.511
^{58}Ni	1.3	1.2	0.353
^{96}Zr	3.7	2.3	3.297
^{96}Ru	0.79	2.3	1.359
^{100}Mo	3.24	—	3.165
^{104}Ru	3.4	—	2.975
^{106}Cd	0.6	—	2.007
^{112}Sn	1.01	—	2.757
^{116}Cd	5.6	—	5.268
^{124}Sn	5.4	—	6.703
^{128}Te	4.3	—	6.159
^{130}Te	4.2	3.5	6.422
^{144}Sm	0.5	1.5	4.749
^{148}Nd	4.8	—	6.929
^{154}Sm	2.2	3.0	5.643
^{160}Gd	5.8	—	5.639
^{176}Yb	8.0	3.6	6.214
^{232}Th	5.4	5.5	7.678
^{238}U	5.8	5.0	7.822

The Bethe neutron excess function might be one of the measure of the outer neutron excess and it can indicate rather simply the halo nuclei on the basis of the neutron and proton density distributions given inside the core of the nucleus. This is very convenient from a theoretical point of view. The excess function is correlated with the halo factor introduced in Ref. [7, 8] as shown in figure 6 (see also [10–12]).

REFERENCES

[1] H.A. Bethe, *Ann. Rev. Nucl. Sci.* **21**, 93 (1970).

[2] A. Bohr, B.R. Mottelson, *Nuclear Structure*, vol. I *Single–Particle Motion*, ed. W.A. Benjamin, Inc., New York, Amsterdam 1969.

[3] P. Möller, J.R. Nix, W.D. Myers, W.J. Swiatecki, *Atomic Data Nucl. Data Tables* **59**, 185 (1995).

[4] Y.K. Gambhir, P. Ring, A. Thimet, *Ann. Phys.* **198**, 132 (1990).

[5] P. Ring, *Prog. Part. Nucl. Phys.* **37**, 193 (1996).

[6] G. Lalazissis, J. König, P. Ring, *Phys. Rev.* **C55**, 540 (1996).

[7] P. Lubiński, J. Jastrzębski, A. Trzcińska, W. Kurcewicz, F.J. Hartmann, R. Schmidt, T. von Egidy, R. Smolańczuk, S. Wycech, *Phys. Rev.* **C57**, 2962 (1998).

[8] R. Schmidt, F.J. Hartmann, B. Ketzer, T. von Egidy, T. Czosnyka, J. Jastrzębski, M. Kisieliński, P. Lubiński, L. Pieńkowski, A. Trzcińska, B. Kłos, R. Smolańczuk, S. Wycech, W. Pöschl, K. Gulda, W. Kurcewicz, E. Widmann, *Phys. Rev.* **C60**, 054309 (1999).

[9] J. Dobaczewski, P. Magierski, W. Nazarewicz, W. Satuła, Z. Szymański, *Phys. Rev.* **C63**, 024308 (2001).

[10] A. Baran, K. Pomorski, M. Warda, *Z. Phys* **A357**, 33 (1997).

[11] S. Wycech *et al.*, *Phys. Rev.* **C54**, 1832 (1996).

[12] Y.K. Gambhir, A.A. Bhagwat, *Phys. Rev.* **C66**, 034306 (2002).